

Detection of Folate Binding Protein with Enhanced Sensitivity Using a Functionalized Quartz Crystal Microbalance Sensor

Walter A. Henne,[†] Derek D. Doorneweerd,[†] Joonhyung Lee,[‡] Philip S. Low,[†] and Cagri Savran^{*§}

Department of Chemistry, School of Chemical Engineering, and School of Mechanical Engineering and Birc Nanotechnology Center, Purdue University, West Lafayette, Indiana 47907

In this report, we describe the development of a quartz crystal microbalance biosensor for detection of folate binding protein (FBP). Using a simple folate–BSA conjugate adsorbed onto a Au-coated quartz sensor, a detection limit of 30 nM was achieved. Binding of FBP to the sensor surface could be blocked at concentrations as high as 1 μ M with a 100-fold excess of folic acid, indicating the specificity of the folate–FBP interaction and the absence of nonspecific binding to the functionalized surface. Moreover, capture could be achieved in the presence of blood serum, making the assay amenable to the analysis of bodily fluids. Further signal enhancement based on an anti-FBP antibody and protein-A-coated gold nanosphere sandwich assay extended the detection limit to 50 pM (~3 orders-of-magnitude improvement). Given the overexpression of FBP in certain malignancies and inflammatory disorders, we expect the methodology described here to be useful to detect FBP as a possible biomarker for disease diagnosis.

The folate receptor (FR), also known as folate binding protein (FBP), is associated with numerous malignancies, including myelogenous leukemias; ovarian, lung, kidney, and breast cancers; and activated immune cells present in chronic inflammatory conditions.^{1–8} Interest in the exploitation of FBP as species for targeted therapy has led to a rapid increase in the development

of folate-targeted drugs, imaging agents, proteins, and systems for the treatment and diagnosis of the above disorders.^{4,7,9–16}

FBP exists as a family of proteins (FR- α , FR- β , and FR- γ) encoded by three unique genes, which are related by ~70% sequence identity. FR- α and FR- β are attached to cell surfaces by a glycosylphosphatidylinositol (GPI) anchor, whereas FR- γ is thought to be a secretory protein.^{17–24} Disengagement from the cell surface, in the case of FR- α and FR- β , can occur via phospholipase cleavage of the GPI anchor or by proteolytic activity.^{22,23} Although folate (Figure 1C) binds with high affinity ($K_d = 10^{-9}$ – 10^{-10} M)²⁵ in a 1:1 stoichiometry to its cognate receptor, most cells obtain folate using other low-affinity pathways (e.g., reduced folate carrier); accordingly, very little FBP is present in normal tissues.^{6,17,26}

FBP has been isolated from bodily fluids, including blood, urine, milk, ascitic fluid, and amniotic fluid, and from the culture media of folate-receptor-positive tumor cell lines, indicating an association between the presence of free folate binding protein and certain malignant cell types.^{6,18,26–30} Furthermore, levels of

* To whom correspondence should be addressed. Tel: 765-494-8601. Fax: 765-494-0539. E-mail: savran@purdue.edu.

[†] Department of Chemistry.

[‡] School of Chemical Engineering.

[§] School of Mechanical Engineering and Birc Nanotechnology Center.

- (1) Westerhof, G. R.; Jansen, G.; van Emmerik, N.; Kathmann, I.; Rijkse, G.; Jackman, A. L.; Schornagel, J. H. *Cancer Res.* **1991**, *51*, 5507–5513.
- (2) Weitman, S. D.; Lark, R. H.; Coney, L. R.; Fort, D. W.; Frasca, V.; Zurawski, V. R., Jr.; Kamen, B. A. *Cancer Res.* **1992**, *52*, 3396–3401.
- (3) Rochman, H.; Selhub, J.; Karrison, T. *Cancer Detect. Prev.* **1985**, *8*, 71–75.
- (4) Paulos, C. M.; Turk, M. J.; Breur, G. J.; Low, P. S. *Adv. Drug Delivery Rev.* **2004**, *56*, 1205–1217.
- (5) Nakashima-Matsushita, N.; Homma, T.; Yu, S.; Matsuda, T.; Sunahara, N.; Nakamura, T.; Tsukano, M.; Ratnam, M.; Matsuyama, T. *Arthritis Rheum.* **1999**, *42*, 1609–1616.
- (6) Mantovani, L. T.; Miotti, S.; Menard, S.; Canevari, S.; Raspagliesi, F.; Bottini, C.; Bottero, F.; Colnaghi, M. I. *Eur. J. Cancer* **1994**, *30A*, 363–369.
- (7) Low, P. S.; Antony, A. C. *Adv. Drug Delivery Rev.* **2004**, *56*, 1055–1058.
- (8) Franklin, W. A.; Waintrub, M.; Edwards, D.; Christensen, K.; Prendegast, P.; Woods, J.; Bunn, P. A.; Kolhouse, J. F. *Int. J. Cancer Suppl.* **1994**, *8*, 89–95.

- (9) Leamon, C. P.; Parker, M. A.; Vlahov, I. R.; Xue, L. C.; Reddy, J. A.; Vetzal, M.; Douglas, N. *Bioconjugate Chem.* **2002**, *13*, 1200–1210.
- (10) Leamon, C. P.; Low, P. S. *Proc. Natl. Acad. Sci. U.S.A.* **1991**, *88*, 5572–5576.
- (11) Leamon, C. P.; Low, P. S. *J. Drug Targeting* **1994**, *2*, 101–112.
- (12) Ke, C. Y.; Mathias, C. J.; Green, M. A. *Adv. Drug Delivery Rev.* **2004**, *56*, 1143–1160.
- (13) Kennedy, M. D.; Jallad, K. N.; Thompson, D. H.; Ben-Amotz, D.; Low, P. S. *J. Biomed. Opt.* **2003**, *8*, 636–641.
- (14) Leamon, C. P.; DePrince, R. B.; Hendren, R. W. *J. Drug Targeting* **1999**, *7*, 157–169.
- (15) Leamon, C. P.; Low, P. S. *Biochem. J.* **1993**, *291*, 855–860.
- (16) Leamon, C. P.; Reddy, J. A. *Adv. Drug Delivery Rev.* **2004**, *56*, 1127–1141.
- (17) Elnakat, H.; Ratnam, M. *Adv. Drug Delivery Rev.* **2004**, *56*, 1067–1084.
- (18) Elwood, P. C. *J. Biol. Chem.* **1989**, *264*, 14893–14901.
- (19) Lacey, S. W.; Sanders, J. M.; Rothberg, K. G.; Anderson, R. G.; Kamen, B. A. *J. Clin. Invest.* **1989**, *84*, 715–720.
- (20) Sadasivan, E.; Rothenberg, S. P. *J. Biol. Chem.* **1989**, *264*, 5806–5811.
- (21) Shen, F.; Wu, M.; Ross, J. F.; Miller, D.; Ratnam, M. *Biochemistry* **1995**, *34*, 5660–5665.
- (22) Antony, A. C.; Verma, R. S.; Unune, A. R.; LaRosa, J. A. *J. Biol. Chem.* **1989**, *264*, 1911–1914.
- (23) Luhrs, C. A.; Slomiany, B. L. *J. Biol. Chem.* **1989**, *264*, 21446–21449.
- (24) Shen, F.; Ross, J. F.; Wang, X.; Ratnam, M. *Biochemistry* **1994**, *33*, 1209–1215.
- (25) Antony, A. C. *Annu. Rev. Nutr.* **1996**, *16*, 501–521.
- (26) Eichner, E. R.; McDonald, C. R.; Dickson, V. L. *Am. J. Clin. Nutr.* **1978**, *31*, 1988–1992.
- (27) Elwood, P. C.; Kane, M. A.; Portillo, R. M.; Kolhouse, J. F. *J. Biol. Chem.* **1986**, *261*, 15416–15423.

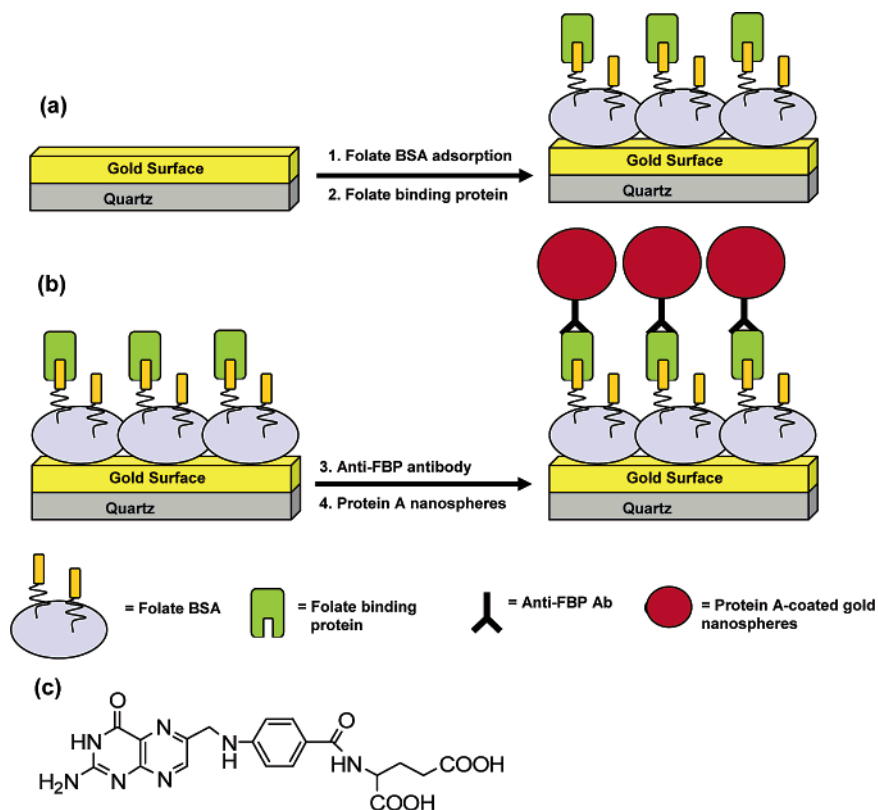


Figure 1. Schematic illustration of sensor surface functionalization and assay procedure for the detection of folate binding protein. (a) Folate BSA (BSA containing ~ 10 folates (0.2 mg/mL)) is adsorbed on the QCM gold sensor surface and used as a receptor to capture FBP. (b) Signal enhancement is obtained by addition of anti-FBP antibody, followed by subsequent protein-A-coated gold nanoparticles. Additional mass from the binding of the anti-FBP and protein-A-coated gold nanoparticles to FBP enabled a detection limit of 50 pM of FBP. (c) Structure of folic acid.

FBP in metastatic disease can increase to 650 $\mu\text{g/mL}$ (22 pM).²⁶ Given that normal serum is virtually free of FBP, elevated FBP levels may serve as a useful clinical biomarker for specific disease states.^{17,26} However, the use of ultrasensitive, real-time analytical systems for detection of FBP remains limited.

Current serum FBP detection strategies consist primarily of radioimmunoassays, given that low levels of FBP are present in both normal and metastatic disease; however, these methods involve long analysis times and the use of hazardous radioactive labels.^{26,30,31} Alternatively, a quartz crystal microbalance (QCM) is a useful analytical method to assess surface layer phenomena, such as self-assembled monolayers, antigen–antibody recognition, and whole bacteria and viral cell capture.^{32–38} Moreover, the methodology is simple and robust, allows real-time detection, and does not require the use of harmful chemicals, such as radiolabeled ligands or expensive chromophoric substrates.

- (28) Hansen, S. I.; Holm, J.; Hoier-Madsen, M. *Biosci. Rep.* **1989**, *9*, 93–97.
 (29) Holm, J.; Hansen, S. I.; Hoier-Madsen, M. *Biosci. Rep.* **1990**, *10*, 79–85.
 (30) Holm, J.; Hansen, S. I.; Hoier-Madsen, M.; Helkjaer, P. E.; Bzorek, M. *APMIS* **1995**, *103*, 663–670.
 (31) Holm, J.; Hansen, S. I.; Hoier-Madsen, M.; Helkjaer, P. E.; Bzorek, M. *APMIS* **1995**, *103*, 862–868.
 (32) Carmon, K. S.; Baltus, R. E.; Luck, L. A. *Anal. Biochem.* **2005**.
 (33) Carter, R. M.; Mekalanos, J. J.; Jacobs, M. B.; Lubrano, G. J.; Guilbault, G. *J. Immunol. Methods* **1995**, *187*, 121–125.
 (34) Eun, A. J.; Huang, L.; Chew, F. T.; Li, S. F.; Wong, S. M. *J. Virol. Methods* **2002**, *99*, 71–79.
 (35) Janshoff, A.; Steinem, C. *Methods Mol. Biol.* **2005**, *305*, 47–64.
 (36) Pavlov, V.; Willner, I.; Dishon, A.; Kotler, M. *Biosens. Bioelectron.* **2004**, *20*, 1011–1021.
 (37) Su, X. L.; Li, Y. *Biosens. Bioelectron.* **2004**, *19*, 563–574.

Basic QCM operation is described by the Sauerbrey relation (eq 1) where a mass change (Δm) of the crystal results in a subsequent change in its resonance frequency (Δf). Here C_{QCM} (17.7 $\text{ng cm}^{-2} \text{Hz}^{-1}$) is the mass sensitivity constant, and n ($= 1, 3, \dots$) is the overtone number.

$$\Delta m_{\text{QCM}} = -(C_{\text{QCM}}/n)\Delta f \quad (1)$$

Therefore, a mass change of the crystal resulting from the association or dissociation of a protein (i.e., FBP) to the quartz sensor surface results in a frequency decrease or increase, respectively.

Selective capture of an analyte by a functionalized crystal surface increases the effective surface mass, and the ensuing decrease in resonance frequency allows measurement of the binding event. Inherent in the nature of quartz crystal microbalance analyses, however, are limitations imposed by surface coverage of the capture ligand and the molecular weight of the analyte of interest. Thus, the use of secondary ligands (e.g., functionalized gold or iron particles) that can bind or “piggyback” onto the already captured analyte can add effective mass to the surface and increase sensitivity by orders of magnitude.³⁹

Here, we report a new approach for rapid, simple detection of folate binding protein, a potential cancer marker, in liquid using

- (38) Uzawa, H.; Kamiya, S.; Minoura, N.; Dohi, H.; Nishida, Y.; Taguchi, K.; Yokoyama, S.; Mori, H.; Shimizu, T.; Kobayashi, K. *Biomacromolecules* **2002**, *3*, 411–414.
 (39) Mao, X.; Yang, L.; Su, X. L.; Li, Y. *Biosens. Bioelectron.* **2006**, *21*, 1178–1185.

quartz crystal microbalance analysis. Our experimental process involved the immobilization of folic acid on a gold-coated QCM sensor surface using bovine serum albumin (BSA) as a spacer/chemisorption species. This method avoided the need to develop complex self-assembled monolayers, thus allowing straightforward, complete surface functionalization in a relatively short period of time. Furthermore, preparation of the capture ligand was simple and inexpensive. To confirm selectivity and to enhance signal, a "piggyback" strategy was developed using antibodies against folate binding protein (anti-FBP) and protein-A-coated gold nanospheres. In this fashion, we significantly increased the sensitivity of the assay by lowering the FBP detection limit to 50 pM (~3 orders-of-magnitude improvement).

EXPERIMENTAL SECTION

Chemicals and Materials. Folic acid, bovine serum albumin (BSA), and concentrated phosphate buffered saline were purchased from Sigma-Aldrich (Saint Louis, MO). 1-Ethyl-3-(3-dimethylaminopropyl) carbodiimide hydrochloride (EDC) and the Bicinchoninic Acid (BCA) Protein Assay kit were purchased from Pierce Biotechnology, Inc. (Rockford, IL). Folate binding protein was purchased from Scripps Research Institute (La Jolla, CA) and was used as supplied. A polyclonal rabbit anti-human folate receptor alpha (anti-FR α) was obtained from Endocyte Inc. (West Lafayette, IN). Protein-A-coated gold nanospheres (20 nm) were purchased from BB International (Cardiff, UK). Molecular weight cutoff spin filters (10 Kd) were purchased from Millipore Corporation (Bellieria, MA). Fresh mouse serum, derived from pelleted whole blood, was obtained via a periorbital bleed from an 8-week-old Balb/C mouse in accordance with Purdue animal care guidelines.

Equipment. The D300 QCM unit (including a temperature controlled fluidic chamber and a data acquisition board/computer), 5-MHz AT-cut optically polished gold-coated quartz crystals i.e., sensor chips, and a UV/ozone chamber were purchased from Q-sense (Västra Frölunda, Sweden) and used according to the manufacturer's instructions without modifications. Data acquisition and analysis were performed using Q-Soft and Q-Tools software packages.

Conjugation of Folic Acid to Bovine Serum Albumin. Folic acid (2.5 mg, 5.6 μ mol) was dissolved in 250 μ L of PBS, and the pH was adjusted to 7 by careful addition of 1 M NaOH. To this solution, EDC (1.1 mg, 5.6 μ mol) was added and stirred in the dark for 30 min. After 30 min, BSA (25 mg, 0.4 μ mol) was dissolved in 750 μ L of PBS (pH 7.4), added to the activated folic acid solution, and stirred for 2 h at room temperature. The BSA conjugate was separated from all low molecular weight materials with a 10-kD molecular weight cutoff spin filter with multiple washes of PBS per the manufacturer's instructions. Protein concentration was determined using a BCA assay and diluted with PBS to a concentration of 10 mg/mL. The number of folate molecules conjugated to each molecule of BSA was assessed by determining the absorbance of the folate conjugate at 363 nm (folic acid: $\epsilon = 6500 \text{ cm}^{-1} \text{ M}^{-1}$ at pH 7.0).

General QCM Setup. New gold-coated sensor chips were sequentially rinsed with Nanopure water and absolute ethanol and then dried under a nitrogen stream. The chips were next placed in a UV/ozone chamber for ~20 min, rinsed with Nanopure water, and again dried under a nitrogen stream. Repeated experiments

with sensors cleaned in this fashion showed similar folate BSA coating patterns without any loss in reproducibility or sensitivity. A freshly cleaned chip was mounted into the QCM chamber according to the manufacturer's instructions and allowed to equilibrate in PBS (pH ~ 7.4) until a stable third overtone frequency (as suggested by the manufacturer) was observed (± 1 Hz over 10 min). This procedure was typically accomplished in 20–30 min. Folate–BSA (0.2 mg/mL) was then allowed to flow into the measurement chamber via gravity-induced smooth flow with multiple additions until the frequency stabilized (± 1 Hz over 10 min). The sensor surface was then rinsed with PBS to remove free and loosely bound folate–BSA.

Capture and Analysis of Folate Binding Protein. Folate binding protein was assayed by introduction of the respective FBP (1–1000 nM) solution into the flow chamber containing the folate–BSA functionalized sensor. Upon signal leveling, the sensor was rinsed with PBS, and the signal was monitored for any changes associated with loosely adsorbed material. FBP specificity was determined using a competitive assay. FBP was preincubated (offline) in the presence of a 100-fold excess of folic acid in PBS (pH = 7.4) and allowed to incubate for 30 min. This folate-competed FBP control was analyzed prior to the introduction of the free FBP, and PBS rinse steps were used between the introduction of each respective test analyte. Further identification and signal enhancement using antibodies against folate binding protein (anti-FBP) was performed using 30 nM anti-FBP antibody and protein-A-coated gold nanospheres diluted 100 \times from the manufacturer's stock solution (stock solution: approximate concentration of protein A was 10 μ g/mL, approximate number of gold nanospheres was 2×10^{12} /mL, and approximate number of protein A moieties per gold nanospheres was 64).

RESULTS AND DISCUSSION

Detection and Specificity of Folate Binding Protein Capture. Figure 1a and b illustrate QCM surface functionalization, the assay procedures of FBP capture, and the subsequent antibody and gold nanosphere signal enhancement strategies. Owing to free gamma and alpha terminal carboxylic acid moieties (Figure 1c), folic acid can readily be conjugated to a free amine, forming a stable amide linkage. Accordingly, folate-conjugated bovine serum albumin (folate–BSA) was synthesized using standard carbodiimide coupling chemistry (~10 folate residues per BSA molecule) and purified by size-exclusion spin filters. The gold-coated QCM sensor was functionalized with folate–BSA (0.2 mg/mL) using successive additions until a stable baseline was observed and no additional frequency change was noted with further folate–BSA additions. We have found that this functionalization strategy can be performed rapidly (~20 min), yielding a surface characterized by minimal nonspecific binding, as evidenced by the absence of FBP binding in the presence of excess free folic acid. Moreover, we have witnessed no significant desorption of the folate–BSA coating over and above the time course of this relatively short assay. QCM surfaces functionalized in this fashion in advance or stored for longer periods of time, however, may require covalent attachment of ligands to the gold surface to enhance long term stability. In Figure 2, a frequency vs time plot demonstrating the initial surface functionalization with folate–BSA is shown. In step 1, immobilization of folate BSA (0.2 mg/mL) in PBS occurs rapidly and irreversibly, as evidenced by

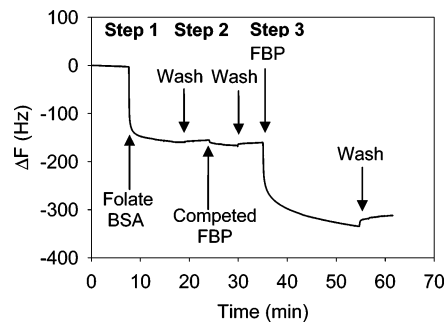


Figure 2. Sensor response indicating FBP binding to folate-BSA. Frequency decrease represents an increase in effective mass of the sensor crystal. Specificity of the capture event was demonstrated by analyzing folate binding protein (1 μM) in the presence of excess folic acid (100 μM). Only a negligible change in signal (~ 1.5 Hz before and ~ 0 Hz after PBS wash) of the competed as compared to noncompeted FBP (~ 150 Hz) indicated specific capture and detection of FBP.

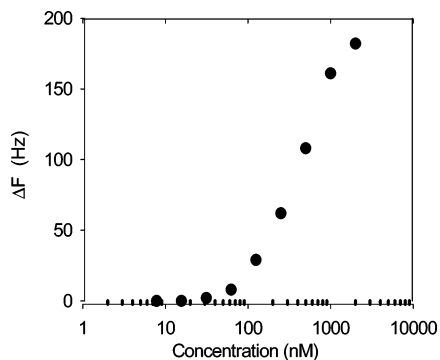


Figure 3. Binding of FBP to folate BSA on QCM surface at varying FBP concentrations (7.5 nM to 2 μM).

a 155 Hz signal change (914.5 ng/cm^2 according to eq 1 with $n = 3$), followed by a minor response after a PBS buffer wash. This latter change is attributed to loosely adsorbed folate BSA on the functionalized surface, which is readily removed by the PBS rinse, whereas the initial signal change is indicative of added mass on the sensor surface following the adsorption of folate-BSA to the gold surface. Sequential folate BSA additions provided no additional effective mass change indicated by the absence of a frequency response; thus, the surface was considered completely coated at this stage.

In step 2 (Figure 2), a control was used to assess nonspecific binding of FBP to the folate-BSA-functionalized surface and to demonstrate FBP capture specificity. Given that FBP binds to folic acid in a 1:1 stoichiometry with high affinity, preincubation of FBP with a large excess of free folic acid is expected to block all free receptor sites and, hence, lead to complete abrogation of FBP binding. Folate binding protein was mixed with a 100-fold excess of free folic acid and analyzed for binding to the folate BSA functionalized sensor. A very minor (~ 1.5 Hz) frequency shift (Figure 2) was detected at an FBP concentration of 1 μM (at an excess folic acid concentration of 100 μM), which was restored after a buffer wash. Because 1 μM FBP approaches our maximal limit of detection due to complete folate ligand saturation (as evidenced by a concentration dependence plot, see Figure 3), the ability to demonstrate complete competition at this high concentration (10 000-fold higher than concentrations of interest) confirmed that interference from nonspecific binding of FBP to the

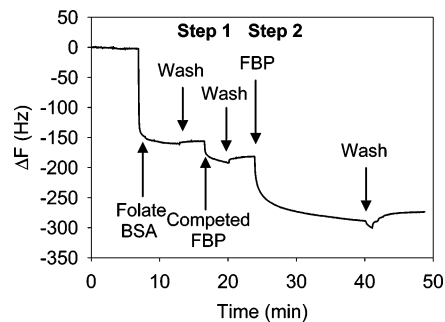


Figure 4. FBP detection in the presence of serum. Competed FBP injection (1000 nM FBP in the presence of 100-fold excess free folic acid) revealed an ~ 30 -Hz signal due to nonspecific binding, whereas addition of noncompeted FBP (1000 nM) led to a signal change of 120 Hz.

sensor surface was insignificant. After a PBS rinse step, a 1 μM solution of folate binding protein (step 3) was analyzed, revealing a frequency response of ~ 150 Hz (885.0 ng/cm^2). Together, these results indicate specific recognition and capture of folate binding protein by the folate-BSA-functionalized QCM sensor with negligible nonspecific binding.

Concentration Dependence of Sensor Response. Figure 3 demonstrates the variation of binding response versus FBP concentration. The response is similar to a Langmuir isotherm, indicating a possible surface saturation above 2000 nM. The lowest detectable FBP concentration without additional signal enhancement was 30 nM. The binding affinity appeared to be lower than the binding affinity in solution. This is expected, since the binding event occurs on a surface where the ligands are not able to move freely to assume optimal positions/orientations for target capture.

Detection of Folate Binding Protein in the Presence of Serum. A major concern inherent in protein detection assays is the possibility of background interference from other chemical species. Given that folate binding protein can slough off from folate receptor positive cancer cells into the blood stream, it was important to assess the impact serum proteins would have in this FBP detection strategy (Figure 4). To this end, mouse serum (diluted 10-fold with PBS) was spiked with FBP (FBP = 1000 nM final concentration) and assayed as outlined above. Upon addition of competed FBP (1000 nM FBP plus 100-fold excess free folic acid) in step 1, we noted a much greater signal change than with FBP in the absence of serum (~ 30 vs 1.5 Hz). This change was attributed to some nonspecific binding of proteins present in the mouse serum. Addition of noncompeted FBP (1000 nM) to the system produced (step 2) a signal of ~ 120 Hz (708.0 ng/cm^2). These data demonstrate the feasibility of detecting FBP in the presence of serum; however, further steps to minimize serum protein interference are necessary.

Signal Enhancement with Anti-FBP Antibody and Protein-A-Coated Gold Nanospheres. Although the above initial experiments were performed to explore the capability for capture and detection of FBP without additional amplification, further studies were explored to improve detection sensitivity. For this purpose, we developed a "piggyback" assay based on the use of an antibody against FBP (anti-FBP) with subsequent addition of protein-A-coated gold nanospheres. In Figure 5a, FBP was first captured (step 1) on the folate-derivatized sensor surface (30 nM), after which anti-FBP antibody (30 nM concentration) was added to the

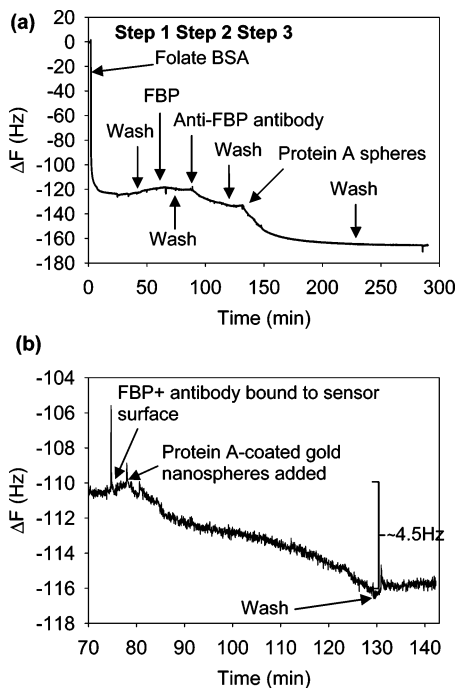


Figure 5. Folate binding protein signal amplification using antibodies against FBP (anti-FBP) and protein-A-coated gold nanospheres. (a) FBP (30 nM) was added to the system, followed by subsequent additions of anti-FBP antibody and protein A nanospheres. PBS washes were performed between steps. (b) Detection of 50 pM FBP using antibody/protein A nanosphere signal enhancement.

system (step 2). As a control, anti-FBP antibody (30 nM) and protein A nanospheres were analyzed prior to addition of FBP, with no signal change noted (data not shown).

Upon addition of folate binding protein to the sensor chamber, a 1.5-Hz (8.85 ng/cm^2) frequency shift was noted at a concentration of 30 nM (step 1). After a PBS rinse and subsequent addition of anti-FBP, a frequency shift of $\sim 13 \text{ Hz}$ (76.7 ng/cm^2) was apparent, indicating an additional increase in crystal mass (step 2). Further signal enhancement was achieved by introduction of protein-A-coated gold nanospheres. Protein A binds to the Fc portion of antibodies; therefore, in addition to the added weight of the protein A component, the attached gold nanosphere greatly

amplifies the mass present on the sensor surface. The addition of FBP, followed by the anti-FBP antibody, and subsequent protein-A-coated nanospheres ($50 \mu\text{L}/5000 \mu\text{L}$) led to total signal change of 45 Hz (265.5 ng/cm^2) (step 3). Using the anti-FBP/protein A nanosphere signal enhancement, we were able to effectively reduce the level of detection from 30 nM (FBP alone) to 50 pM (Figure 5b), which approached clinically relevant concentrations.

CONCLUSIONS

Given the therapeutic potential for folate-targeted drugs and imaging agents, rapid diagnostic systems capable of detecting folate binding protein are necessary for diagnosis, staging, and monitoring of therapies associated with folate delivery.^{7,9–11,14–16} In tandem with selective delivery of folate conjugates, new test systems will undoubtedly be needed to establish whether specific cancers express the level of folate receptor necessary for treatment with the established folate-targeted treatment modalities. Since folate binding protein may serve as a useful biomarker for appropriate drug selection, assessment of metastasis, and general detection of cancer and inflammatory diseases, we have devised a quartz crystal microbalance sensing platform for simple, fast detection of this important protein. Here, we describe for the first time the use of QCM sensors for the direct capture and detection of folate binding protein using a folate-functionalized sensor. Folate-derivatized BSA provided a simple capture ligand, which could be rapidly and efficiently immobilized on the gold surface of the QCM biosensor. Furthermore, specificity and signal improvement were achieved using an antibody against FBP followed by addition of protein-A-coated gold nanospheres. Using this “piggyback” strategy, we anticipate the application of our methodology to numerous sensor surfaces, including nanomechanical cantilever sensors and arrays. Thus, future work will explore these systems to expand and enhance detection capabilities.

ACKNOWLEDGMENT

We thank Endocyte Inc. for providing the anti-FBP antibody.

Received for review February 21, 2006. Accepted April 24, 2006.

AC060324R